Slowly expanding lesions relate to persisting black-holes and clinical outcomes in relapse-onset multiple sclerosis

Alberto Calvi [a,*], Carmen Tur [a,b], Declan Chard [a], Jonathan Stutters [a], Olga Ciccarelli [a], Rosa Cortese [c], Marco Battaglini [c], Anna Pietroboni [d,e], Milena De Riz [d,e], Daniela Galimberti [d,e], Elio Scarpini [d,e], Nicola De Stefano [c], Ferran Prados [a,f,g], Frederik Barkhof [a,f,h]

[a] Queen Square MS Centre, Department of Neuroinflammation, Institute of Neurology, Faculty of Brain Sciences, University College London (UCL), United Kingdom
[b] Neurology-Neuroimmunology Department, Multiple Sclerosis Centre of Catalonia (Cemcat), Vall d'Hebron Barcelona Hospital Campus, Barcelona, Spain
[c] Dep. of Medicine, Surgery and Neuroscience, University of Siena, Italy
[d] Fondazione IRCCS Ca' Granda Ospedale Maggiore Policlinico, University of Milan, Italy
[e] Department of Biomedical, Surgical and Dental Sciences, University of Milan, Centro Dino Ferrari, Milan, Italy
[f] Centre for Medical Image Computing (CMIC), Department of Medical Physics and Biomedical Engineering, University College London, London, United Kingdom
[g] e-Health Centre, Universitat Oberta de Catalunya, Barcelona, Spain
[h] Radiology & Nuclear Medicine, VU University Medical Centre, Amsterdam, The Netherlands

ARTICLE INFO

ABSTRACT

Background: Slowly expanding lesions (SELs) are MRI markers of chronic active lesions in multiple sclerosis (MS). T1-hypointense black holes, and reductions in magnetization transfer ratio (MTR) are pathologically correlated with myelin and axonal loss. While all associated with progressive MS, the relationship between these lesion's metrics and clinical outcomes in relapse-onset MS has not been widely investigated.

Objectives: To explore the relationship of SELs with T1-hypointense black holes, and longitudinal T1 intensity contrast ratio and MTR, their correlation to brain volume, and their contribution to MS disability in relapse-onset patients.

Methods: 135 patients with relapsing-remitting MS (RRMS) were studied with clinical assessments and brain MRI (T2/FLAIR and T1-weighted scans at 1.5/3 T) at baseline and two subsequent follow-ups; a subset of 83 patients also had MTR acquisitions. Early-onset patients were defined when the baseline disease duration was $\leq$ 5 years (n = 85). SELs were identified using deformation field maps from the manually segmented baseline T2 lesions and differentiated from the non-SELs. Persisting black holes (PBHs) were defined as a subset of T2 lesions with a signal below a patient-specific grey matter T1 intensity in a semi-quantitative manner. SELs, PBH counts, and brain volume were computed, and their associations were assessed through Spearman and Pearson correlation. Clusters of patients according to low (up to 2), intermediate (3 to 10), or high (more than 10) SEL counts were determined with a Gaussian generalised mixture model. Mixed-effects and logistic regression models assessed volumes, T1 and MTR within SELs, and their correlation with Expanded Disability Status Scale (EDSS) and confirmed disability progression (CDP).

Results: Mean age at study onset was 35.5 years (73% female), disease duration 5.5 years and mean time to last follow-up 6.5 years (range 1 to 12.5); median baseline EDSS 1.5 (range 0 to 5.5) and a mean EDSS change of 0.31 units at final follow-up. Among 4007 T2 lesions, 27% were classified as SELs and 10% as PBHs. Most patients (n = 65) belonged to the cluster with an intermediate SEL count (3 to 10 SELs). The percentage of PBHs was higher in SELs than non-SELs (up to 61% vs 44%, p < 0.001) and within-patient SEL volumes positively correlated with PBH volumes (r = 0.53, p < 0.001). SELs showed a decrease in T1 intensity over time (beta = -0.004, 95%CI −0.005 to −0.003, p < 0.001), accompanied by lower cross-sectional baseline and follow-up MTR. In mixed-effects models, EDSS worsening was predicted by the SEL log-volumes increase over time (beta = 0.11, 95% CI 0.03 to 0.20, p = 0.01), which was confirmed in the sub-cohort of patients with early onset MS (beta = 0.14,

---

95%CI 0.04 to 0.25, p = 0.008). In logistic regressions, a higher risk for CDP was associated with SEL volumes (OR = 5.15, 95%CI 1.60 to 16.60, p = 0.006).

Conclusions: SELs are associated with accumulation of more destructive pathology as indicated by an association with PBH volume, longitudinal reduction in T1 intensity and MTR. Higher SEL volumes are associated with clinical progression, while lower ones are associated with stability in relapse-onset MS.

1. Introduction

Multiple sclerosis (MS) is characterized by multifocal inflammatory demyelinating lesions with variable degrees of neurodegeneration. Lesions in MS have been classified in subtypes (active, remyelinated, chronic active, inactive), reflecting the presence of pathological changes over time (Prineas and Parratt, 2012; Prineas et al., 2001). Newly active lesions subside over days to weeks (Thompson et al., 2018), are followed by variable degrees of remyelination (Barkhof et al., 2003). Some lesions evolve into a chronic active (or mixed active-inactive) stage, characterised by a hypocellular core and activated iron-enriched macrophages-microglia at the lesion border, leading to a radial expansion, further myelin damage, axonal loss, and gliosis (Frischer et al., 2009; Kuhlmann et al., 2017; Prineas et al., 2001). The heterogeneity of the MS clinical spectrum is in part explained by the different distribution of lesion subtypes over the course of the disease (Kuhlmann et al., 2017). Chronic active lesions represent 30% to 50% of the overall lesion burden in pathological studies (Frischer et al., 2009; Lassmann, 2019; Luchetti et al., 2018; Frischer et al., 2015), with higher percentages found in secondary-progressive MS (SPMS) compared to relapsing-remitting MS (RRMS) (Frischer et al., 2009; Frischer et al., 2015). Accumulation of chronic active lesions contribute to persistence of inflammation, chronic demyelination and axonal loss driving disability in MS (Luchetti et al., 2018), and so it is important to identify standardised *in vivo* surrogate markers.

On magnetic resonance imaging (MRI), T2-weighted and fluid-attenuated inversion recovery (FLAIR) sequences sensitively detect all MS lesion subtypes, but they are not specific for any of the histopathological subtypes. Chronic hypointensity on T1-weighted sequences (van Walderveen et al., 1998; Van Waesberghe et al., 1999) and persistently low magnetization transfer ratio (MTR) (Schmierer et al., 2004; Kapoor et al., 2010) values are associated with axonal loss and demyelination. Black holes (BHs) can be defined as lesions with T1 intensity darker than the grey matter (GM) and surrounding tissues (Molyneux et al., 2000). Persisting black holes (PBHs), which generally represent a significant proportion of the overall lesions (20–40%) (van den Elskamp et al., 2008; Bagnato et al., 2003), associate with future disability progression and brain atrophy accrual (Truyen et al., 1996; van Walderveen et al., 2001; Sailer et al., 2001), therefore possibly representing lesions at the end-stage of their evolution. So far, there is no standardised imaging biomarker for chronic active lesions.

Slowly expanding lesions (SELs) are identified through longitudinal deformation analysis using routinely acquired volumetric MRI. Some studies have shown an association between the presence of SELs and the chronic active lesions (Elliott et al., 2017; Dal-Bianco et al., 2017). Compared with manually outlined lesion mask, prone to inter and intra-rater variability (Vrenken et al., 2013), the automated longitudinal computation of a deformation field in SELs allows the acquisition of a quantitative measure of MS lesion expansion, hence it could provide a marker for chronic inflammatory activity to measure the predisposition to develop disability. SELs are seen in all MS phenotypes, but more commonly in the progressive ones and less frequently in RRMS (median 7 vs. 4 per patient, respectively), and they evolve independent of gadolinium enhancement (Elliott et al., 2017). Compared with other lesions, SELs show a progressive decline in T1 intensity suggestive of ongoing neuro-axonal damage (Elliott et al., 2019). In a recent study assessing RRMS and SPMS patients, SELs had a lower MTR and greater radial diffusivity in diffusion-weighted imaging (DWI) from baseline up to 72 weeks (Elliott et al., 2020), consistent with MS-specific chronic demyelination. In a recent study in SPMS (n = 345), definite SEL volume correlated with higher total lesion burden, percentage brain volume reduction and greater reduction in MTR, and associated with greater disability (Calvi et al., 2022). However, it is not known whether such clinical associations also exist in RRMS, nor whether using different thresholds to define a lesion that has expanded, significantly influences those associations.

The aims of this study were: 1) To compute SELs in a relapse-onset observational cohort over a long-term follow-up; 2) To identify whether there is a relationship between PBHs and SELs; 3) To assess changes in lesional T1 intensity contrast ratio (the ratio of mean T1 values in individual lesions divided by the mean GM T1 value) and MTR values within SELs vs. non-SELs; 4) To evaluate whether the increase in number and volume of SELs are associated with worsening disability as assessed by EDSS change over time or higher risk of MS progression.

2. Material and methods

2.1. Participants and MRI acquisitions.

A 2-centre retrospective observational cohort of early relapse-onset patients was selected from a collaborative MAGNIMS initiative between the Queen Square MS Centre (QSMSC) University College London (UK), the University of Siena (Italy) and the University of Milan (Italy). At the beginning of the studies, patients gave written consent for their data to be used in post-hoc studies, which were approved by the local Ethics Committee. The inclusion criteria were the following: a confirmed diagnosis of RRMS according to the revised 2017 McDonald criteria (Thompson et al., 2018) and availability of at least three consecutive MRI longitudinal images (baseline, intermediate follow-up and last follow-up), including FLAIR or T2-weighted scans at baseline, and 3D acquired T1 at all time points, with adequate image quality. For some patients MTR sequences were also available. The scans from the University of Siena were collected on a Gyroscan operating at 1.5 T (Philips Healthcare, Best, the Netherlands), while those from the University of Milan were acquired on an Achieva 3 T scanner (Philips, Eindhoven, The Netherlands). The acquisition parameters are shown in Supplementary Material (Table 1). Each patient was scanned consistently with the same machine throughout the trial. An initial number of 139 patients with MS were identified, but data from 4 patients had to be discarded due to image artefacts (final sample n = 135). A subset of 83 patients (provided from University of Siena) also had MTR at baseline and final follow-up, although a machine upgrade meant this could only be analysed cross-sectionally at both timepoints rather than longitudinally between them.

2.2. Clinical assessments.

At each scanning session, patients were also clinically assessed using the Expanded Disability Status Scale (EDSS) (Kurtzke, 1983) score, obtained by an MS specialist. The EDSS change was calculated as the difference between EDSS at last follow-up and EDSS at baseline. Confirmed disability progression (CDP) was defined by an EDSS score change ≥ 1.0 or ≥ 0.5, when baseline EDSS score was < 5.5 or ≥ 5.5 (cut-offs as previously used in phase III trials (Lublin et al., 2016), respectively, which was confirmed in the following 6 months after last follow-up visit.

Table 1

Clinical-demographic and radiological characteristics of the patients enrolled in the study.

Clinical-demographics and radiological features	
n	135
Female n (%)	99 (73 %)
Age at baseline, mean (SD) [years]	35.5 (9.0)
Disease duration at baseline, mean (range) [years]	5.5 (0 – 32.5)
Time to MRI scan follow-up, mean (range) [years]	
- at intermediate follow-up	2.9 (0.4 – 10.5)
- at last follow-up	6.5 (1.0 – 12.5)
EDSS, median (range)	
- at baseline	1.5 (0 – 5.5)
- at last follow-up	2.0 (0 – 8.0)
EDSS change, mean (SD)[a]	0.30 (1.34)
MS phenotype	
- at baseline	RRMS = 135
- at last follow-up	RRMS = 129; SPMS = 6
Number (%) of patients treated[b]	
- at baseline	66 (49%)
- at last follow-up	102 (75%)
Number (%) of patients with CDP[c]	37 (27%)
NAWM volume at baseline [ml], mean (SD)	656.1 (31.2)
CGM volume at baseline [ml], mean (SD)	819.6 (42.1)
DGM volume at baseline [ml], mean (SD)	48.8 (3.6)
NBV at baseline [ml], mean (SD)	1524.5 (59.5)
BPF at baseline, mean (SD)	0.72 (0.03)
PBVC baseline to last follow-up, mean (SD)	−0.18% (0.49)

Abbreviations: SD = standard deviation; EDSS = Expanded Disability Status Scale; CDP = confirmed disability progression; NAWM = normal appearing white matter; CGM = cortical grey matter; DGM = deep grey matter; NBV = normalised brain volume; BPF = brain parenchymal fraction; PBVC = percentage brain volume change.

[a] EDSS change was calculated by subtracting EDSS at last follow-up and EDSS at baseline.

[b] Treatment at baseline: 1st line (n = 54) and 2nd line (n = 12); Treatment at follow-up: 1st line (n = 68) and 2nd line (n = 34).

[c] CDP was defined by an EDSS score increase $\geq$ 1.0 or $\geq$ 0.5, when baseline EDSS score was < 5.5 or $\geq$ 5.5, respectively, and confirmed at least after 6 months after the visit.

2.3. T2 lesion, new T2 lesions, tissue segmentation and SEL detection.

T2 hyperintense lesions were manually identified on the dual-echo T2 or FLAIR baseline images using a semi-automated edge finding tool (JIM v7.0, Xinapse Systems, Aldwincle, UK) and baseline T2 lesion volumes were determined. The original T2 images acquired in 2D with a voxel resolution of (1x1x3) mm^3 were resampled into a 1-mm isotropic space, and lesions were co-registered to the 3D-T1 images using a pseudo-T1 image generated by subtracting the 2 echoes of the T2-weighted sequence (Hickman et al., 2002).

New T2 lesions were assessed at the intermediate and last follow-up sessions, using an in-house algorithm, based on the subtraction of follow-up and the baseline lesion masks segmented by trained observers using local thresholding.

For brain extraction, tissue segmentation and parcellation, Geodesic Information Flows (GIF) was used on the lesion filled T1 scans (3D acquired) (Cardoso et al., 2015), providing the following metrics: normalised brain volume (NBV), normalised normal-appearing white matter (NAWM, i.e. the white matter volume after subtracting the T2 lesion volume), normalised cortical grey matter (CGM) and normalised deep grey matter (DGM) volumes. Lesion-filling was used (a multi-time-point patch-based method) to avoid segmentation bias (Prados et al., 2016). Percent Brain Volume Change (PBVC) from baseline to intermediate follow-up and from baseline to last follow-up, as measure of brain atrophy, was calculated using the SIENA method (Smith et al., 2002).

A recently developed SEL detection algorithm was used, as previously described (Calvi et al., 2022), to identify the subsets of all the candidate SELs, as opposed to the non-SELs. Candidate SELs were further sub-classified as 'definite' based on both the constancy over time and the concentricity of their expansion. The other fraction of expanding lesions among the SEL candidates, not satisfying constancy/concentricity criteria, were designated as 'possible' SELs. The term SEL-derived metrics is used in the text to identify the overall three subsets of lesion types identified with this pipeline (definite SEL, possible SEL and non-SEL).

2.4. T1 Ratios and MTR within lesion types.

The T1-weighted images were registered to the T2-weighted/FLAIR images, in the same space were the lesion masks were drawn. The T1 intensity ratios were calculated according to the image intensity, and they were computed within the lesions referring to the grey matter, i.e. they were obtained from the division of all the T1 values by the mean GM T1 value. In particular, they corresponded to the mean T1 value within the respective lesion mask area, after dividing each value by the patient-specific mean T1 value within the GM (T1 ratio$_{GM}$ = T1$_{LESION}$/ T1$_{GM}$).

The lesion-specific T1 was computed independently at each time point. MTR, in percent unit (pu) was computed at baseline and last follow-up for the subset of patients who had been scanned with the MTR sequence (MT pulse 1.2 ms, radio-frequency field strength 20 μT, field of view 256X256, voxel size 0.97x0.97x3 mm). In consideration of the long time to the last follow-up for most of the MTR subcohort, which included an upgrade of the scanner at University of Siena site, the baseline MTR was discarded from the analysis to avoid any bias. T1 and MTR were analysed after applying the SEL detection algorithm within the SEL-derived metrics at the single lesion level (average values of all the voxels in the specific mask).

2.5. PBH detection

The identification of black holes at each time point was automated based on a voxel-by-voxel analysis of the local T1 ratio$_{GM}$ value within each lesion mask, adopting a previous definition of BH as a region with a signal intensity similar to or reduced relative to the signal intensity of the grey matter (GM) and corresponding to a lesion mask drawn on T2-weighted MRI (van Walderveen et al., 2001). The formula used identified the upper threshold of T1 intensity below which a lesion is classified as a BH:

T1 intensity threshold = mean T1 ratio$_{GM}$ − (SD T1 ratio$_{GM}$)

A further confirmatory step, to avoid inclusion of small artefactual hypointensities, required the T1 hypointense volume to cover an area greater than 10% of the individual lesion volume at all time points to fulfill the classification as a persisting black hole (PBH). The obtained PBHs were manually checked by a neurologist with expertise in imaging (AC) and the doubtful cases reviewed with the neuroradiologist (FB) to ensure accuracy.

2.6. Statistical analysis

Analysis was performed with STATA version 16 and statistical significance reported at $p < 0.05$, while frequency distributions and plots were drawn using R (a language and environment for statistical computing R Core Team [2020]). Differences in EDSS over time between baseline and last follow-up were assessed with the Wilcoxon signed rank test. A descriptive analysis was performed at the lesion level for each lesion type, including the SEL-derived metrics and the hypointense lesions (total BH and PBH) and the frequency distributions were visually assessed. Then, lesion counts, and volumes were analysed at the patient level calculating the sum of the number and volume of the respective lesion types, providing median and interquartile range (IQR) or mean and standard deviation (SD). Each specific lesion volume type was log-transformed (base 10) in order to meet the normality assumption. The

associations were computed with Pearson (for normally ditributed variables, i.e. log-transformed lesion volumes) or Spearman (for non-normally distributed variables, i.e. lesion counts) correlation coefficients. A Gaussian mixture model (GMM) was built in order to identify the underlying components, and to categorise subpopulations of patients according to their total SEL count number, using possible SEL type (Fig. 1, Supplementary Material).

T1 and MTR were anlaysed using a mixed-effects regression model, assessing their values one at a time at a lesion-by-lesion basis as outcome variable; the random effect components included the patient-specific identification number, the study centre and a unique lesion identifier in order to take into account the within-subject variability.

Mixed-effects regression models using as outcome the EDSS, adjusted for MRI conventional measures (baseline total T2 lesion volume and PBVC) were used to assess the relationship with SELs, using the interaction term between each SEL-derived metric (i.e. definite SEL, possible SEL and non-SEL) and the time at follow-up, and the random effects including the patient-level and the time at follow-up. To better explore early onset MS, a filter was introduced in order to identify patients with short disease duration at baseline ($\leq$5 years). This subset of patients, defined 'early onset MS subcohort', was then assessed using a similar mixed-effects regression model to investigate EDSS outcome over time in relation to the SEL-derived metrics, adjusting for the demographic and MRI covariates.

Multiple logistic regressions, adjusted for demographic covariates (age at baseline, gender, time to last follow-up) were applied to investigate the risk of CDP explained by within-patient counts or log-volumes of SELs. The odds ratio (OR) and p values are reported. The performance of the models using conventional MRI or SEL-derived metrics was assessed using the Bayesian information criterion (BIC).

3. Results

3.1. Cohort demographics and clinical features

Patients demographical data and clinical measures are reported in Table 1. Mean disease duration since the initial diagnosis was 5.5 years (range 0 to 32.5) and mean age at study onset was 35.5 years (SD = 9.0). As a multi-centric retrospective study, there was variability of time intervals from the baseline to the subsequent follow-ups MRI scans (mean time at intermediate follow-up 2.9 years, range 0.4 to 10.5; mean time at last follow-up 6.5 years, range 1.0 to 12.5). At baseline, 49% of patients (n = 66) were on any disease modifying treatment (DMT), while at last follow-up 75% used DMTs (n = 102). EDSS had significantly increased at final follow-up compared to baseline (mean EDSS change 0.30, SD 1.34, Wilcoxon signed-rank test, p = 0.035). Overall, 37 patients (27%)

demonstrated CDP and 6 patients (0.4%) had developed SPMS by the end of the study. 85 patients out of 135 (63%) had a short disease duration at sudy onset ($\leq$5 years). The clinical characteristics of the subcohort were the following: 61 were female (71%), mean disease duration at baseline was 1.43 years (range 0 to 4.7) and mean EDSS change 0.11 (SD = 1.40).

3.2. Descriptive analysis of MRI metrics

All MRI metrics at baseline are summarised in Table 2. At the lesion level, a total of 4007 lesions on T2-weighted or FLAIR images were manually segmented, then subclassified as follows: definite SELs (n = 408, ratio to total lesions = 0.10), possible SELs (n = 1061, ratio to total lesions = 0.26), non-SELs (n = 2538, ratio to total lesions = 0.64). The median baseline total lesion count per patient was 23, of which 2 and 6 were classified as definite SELs and possible SELs (9% and 26% out of the

Table 2

Lesion counts and volumes, by SEL types, total BH and PBH at the patient level.

Lesion-specific MRI metrics			
Counts	T2 lesion count at baseline [n], median (IQR)		23 (13 – 41)
	SEL-derived	non-SEL count [n], median (IQR)	13 (6 – 26)
		possible SEL count [n], median (IQR)	6 (3 – 12)
		definite SEL count [n], median (IQR)	2 (1 – 4)
	Total BH count at baseline [n], median (IQR)		6 (3 – 10)
	PBH count [n], median (IQR)		4 (2 – 6)
	New T2 lesions between baseline and intermediate follow-up [n], median (IQR)		4 (1 – 8)
	New T2 lesions between intermediate and last follow-up [n], median (IQR)		3 (1 – 7)
Volumes	T2 lesion volume at baseline [ml], median (IQR)		3.77 (1.56 – 9.74)
	SEL-derived	non-SEL volume [ml], median (IQR)	1.49 (0.45 – 3.81)
		possible SEL volume [ml], median (IQR)	0.89 (0.32 – 2.10)
		definite SEL volume [ml], median (IQR)	0.51 (0.15 – 2.00)
	Total BH volume at baseline [ml], median (IQR)		0.19 (0.09 – 0.50)
	PBH volume at last follow-up [ml], median (IQR)		0.22 (0.08 – 0.69)
	New T2 lesion volume between baseline and intermediate follow-up [ml], median (IQR)		0.23 (0.06 – 0.71)
	New T2 lesion volume between intermediate and last follow-up [ml], median (IQR)		0.22 (0.04 – 0.53)

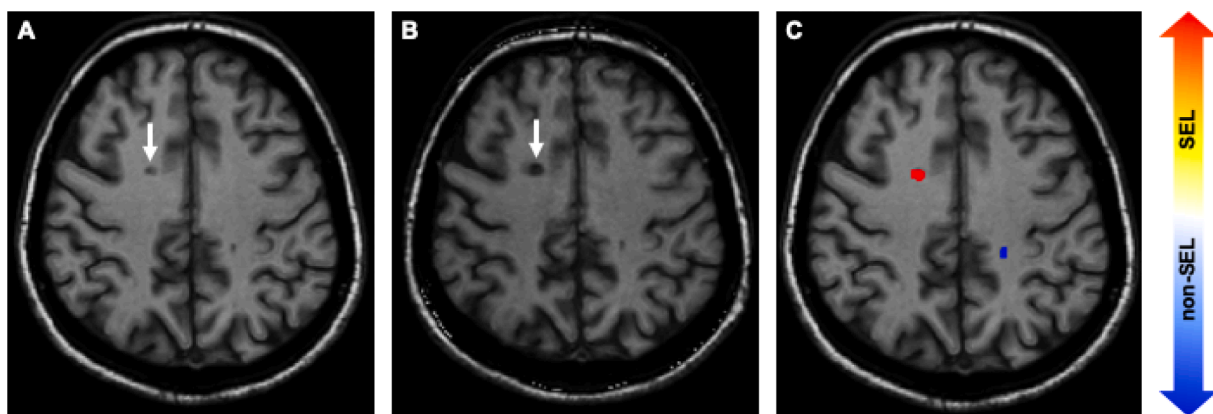**Abbreviations**: BH = black hole, PBH = persisting black hole; IQR = interquartile range.

Fig. 1. Example of patient with SEL and PBH. Example of patient enrolled in the study (53 years old at baseline with RRMS and EDSS 4.5, progressed to 6.0). Image A is the baseline T1-weighted scan, image B is the follow-up scan. The white arrow indicates a lesion that was T1 hypointense at baseline and over a follow-up 9.3 years thus represent a PBH, and in C the Jacobian map indicates that the same lesion corresponds to a SEL.

total lesion count, respectively) and their volume corresponded to 13% and to 24% respectively out of the total lesion volume (Table 2). The within-patient median baseline total BH count was 6, of which 4 were PBHs, and the median new T2 lesion count in the first and second time interval were 4 and 3, respectively. Patients with at least one definite SEL and one possible SEL represented 86% (n = 116) and 99% (n = 133), respectively. At least one PBH was identified in 89% of patients (n = 121).

Global brain and regional brain volumes at baseline, and brain atrophy (PBVC), were consistent with a relapsing-onset MS population (Table 1). An example of a patient showing a PBH, that correspond also to a SEL is shown in Fig. 1.

3.3. High, intermediate and low SEL count clusters

Three clusters based on the SEL count were identified according to the best performance of the GMM model (Supplementary material, Fig. 1), using counts of possible SELs as a reference. Patient clusters were defined as follows: 'low SEL counts' including patients with up to 2 SELs (n = 31 out of 135, 23%); 'intermediate SEL count' with a count ranging from 3 to 10 SELs (n = 65, 48%); 'high SEL count' had > 10 SELs (n = 39, 29%). When differences in demographical and clinical characteristics were analysed according to these SEL count clusters, an higher EDSS at last follow-up was identified in the high SEL count compared to the other patient groups (p = 0.026, Table 2 Supplmentary Materials). The baseline T2 lesion volume and baseline T2 lesion counts were higher in the high SEL count cluster (p < 0.001) while NBV, CGM and DGM were the lowest in this patient group (Table 2, Supplementary Material).

3.4. Associations between new T2 lesions, T1-black holes, PBHs and SELs

At the lesion level, out of the overall T2 lesions (n = 4007), 10% were classified as PBHs (n = 449) and they represented 52% of the total BHs (n = 851). The analysis of the counts of the total BHs and PBHs according to their SEL-derived volumetric category (definite SEL, possible SEL, non-SEL), and the relative percentage of PBHs to the total BHs is presented in Table 3. When divided into the three SEL-derived categories, PBHs were more common among possible and definite SELs, as compared to non-SELs (61% and 52% versus 44%, respectively, Pearson's Chi-squared test, p < 0.001). The highest positive correlations were identified between the baseline total BH counts and possible SEL counts (Spearman rho = 0.48, p < 0.001), between PBH counts and possible SEL counts (Spearman rho = 0.47, p < 0.001), followed by new T2 lesion counts between intermediate and last follow-up and possible SEL counts (Spearman rho = 0.27 p = 0.002). Similarly, the sum of PBH volume at last follow-up positively correlated with possible SEL log-volumes (Pearson r = 0.53, p < 0.001). To confirm that the associations observed were not driven by those with longer interval scanning, the analysis was repeated excluding 17 patients with follow-up times greater than 2 SD from the mean of the cohort (a threshold of 10.6 years) in which the associations observed remained significant.

3.5. Associations between SELs and brain volumes

At baseline and at a patient level, SEL log-volumes were negatively associated with NBV (highest absolute values for possible SEL, Pearson r = -0.35, p < 0.001) and with normalised CGM and DGM volumes

(highest absolute values for possible SEL, Pearson r = -0.41, p < 0.001; r = -0.48, p < 0.001; respectively). Similarly, at last follow-up (possible) SEL log-volumes negatively correlated with NBV (Pearson r = -0.40, p < 0.001) and both CGM and DGM volumes (Pearson r = -0.44, p < 0.001; r = -0.49, p < 0.001). No significant associations in the correlation analysis were found between possible SEL log-volumes and PBVC (Pearson r = 0.02, p = 0.83).

3.6. T1 intensity ratio and MTR within SELs

Definite and possible SELs had lower cross-sectional T1 ratio values compared to non-SELs (Table 4). Longitudinally, T1 intensity ratio decreased over time in both possible and definite SELs while T1 intensity ratio increased within non-SELs. The differences of T1 change between SELs and non-SELs were significant, with the greatest T1 decrease within the possible SELs (-0.004 [95% CI: −0.005 to −0.003], p < 0.001, Fig. 2) when adjusted for demographical (age, gender, time at last follow-up) and MRI covariates (baseline T2 lesion volume and PBVC).

In the subcohort of patients with MTR acquisitions (n = 83), over 2352 lesions 10% (n = 232) were definite SELs, 25% (n = 572) were possible SELs, and 65% non SELs (n = 1548). MTR computed cross-sectionally at baseline and last follow-up was lower within SELs compared to non-SELs (adjusted difference between SEL and non-SEL up to −1.5 percent unit [pu]; at follow-up up to −1.6 [pu]), when adjusted for demographical and MRI covariates (Table 3 Supplementary Material).

3.7. SEL associations to disability (EDSS) over time and risk of progression (CDP)

In the models to predict disability evolution over time using mixed-effects regressions, adjusting for demographic and MRI covariates (age, gender, disease duration, time at follow-up evaluation, total baseline lesion volume and PBVC), EDSS worsening over time was predicted by an increase in SEL (interaction term for possible SEL log-volumes: beta = 0.11, 95%CI 0.03 to 0.20, p = 0.01), when the other MRI variables (baseline total lesion volume and PBVC) were not associated. Using a similar adjusted model within the early onset MS subcohort (n = 85), EDSS was still predicted by an increase in SEL (interaction term for

Table 4
Cross-sectional and longitudinal T1 intensity ratio within lesion types.

Lesion category	T1* baseline (95% CI)	T1* at last follow-up (95% CI)	T1* change beta (95% CI)
Non-SEL (n = 2538)	1.284 (1.234, 1.333)	1.286 (1.236, 1.336)	0.002 (0.002, 0.003) **p < 0.001**
Possible SEL (n = 1061)	1.215 (1.165, 1.264)	1.211 (1.161, 1.261)	−0.004 (-0.005, −0.003) **p < 0.001**
Definite SEL (n = 408)	1.220 (1.169, 1.271)	1.217 (1.166, 1.268)	−0.003 (-0.004, −0.002) **p < 0.001**

*Data were analysed on 4007 lesions and are presented as adjusted mean (95% confidence intervals) obtained from the mixed-effects model taking into account time to follow-up (covariates included were age, gender, baseline T2 lesion volume, PBVC). In bold the significant results set as p-value < 0.05.
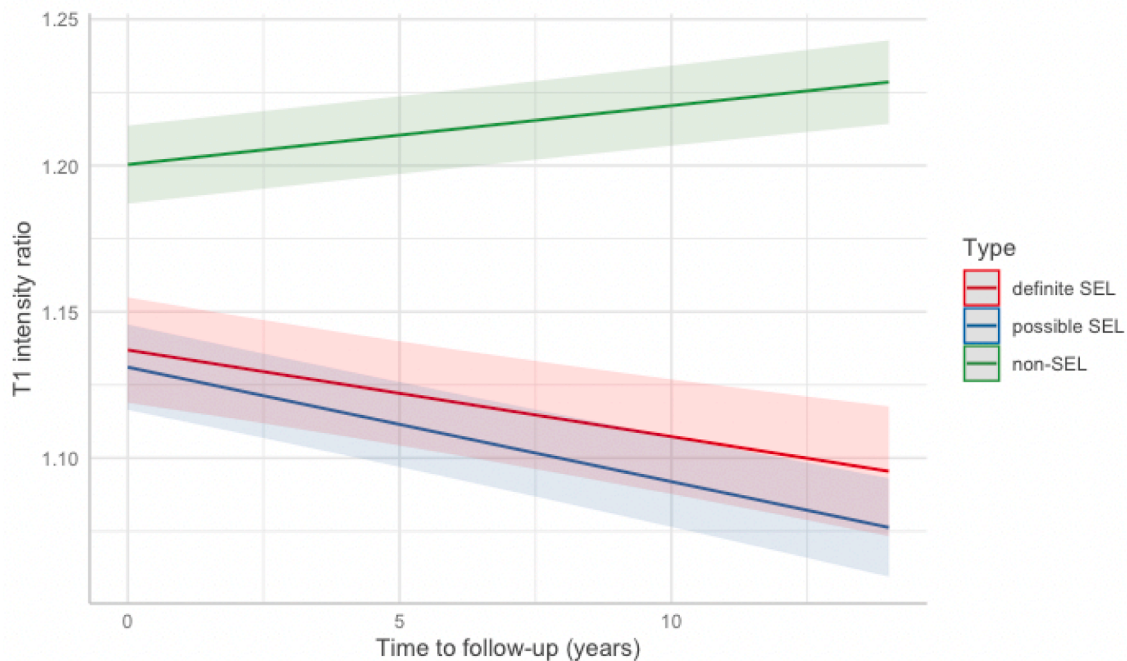
Table 3
Distribution of black holes counts divided by the SEL-derived categories.

	Lesion category	Total BH, count (n = 851)	PBH, count (n = 449)	% PBH over the total BH corresponding category
SEL-derived	Non-SEL	336	147	44%
	Possible SELs	375	229	61%
	Definite SELs	140	73	52%

Abbreviations: BH = black hole, PBH = persisting black hole.

Fig. 2. T1 change over time within SEL-derived lesion metrics. Plot showing the relationship between the predicted T1 intensity ratio change and time at last follow-up from baseline at the lesion level. The lines visualised were drawn on R by plotting the predicted values by the mixed effect model, considering the three lesion categories and showing that SELs (possible and definite) show a T1 reduction compared to non-SELs that have a T1 increase.

possible SEL log-volumes: beta = 0.14, 95%CI 0.04 to 0.25, p = 0.008).

The risk of developing earlier disability was assessed using as outcome the development of CDP over time at the last follow-up. For every additional unit increase in SEL (possible SEL log-volume), when assessed independently (including demographic characteristics), a five-fold higher risk for CDP was found in the logistic regression (OR = 5.15, 95%CI 1.60 to 16.60, p = 0.006, pseudo-R^2 = 0.11). When the other MRI variables were analysed independently, total baseline lesion volume was also independently able to predict CDP, indicating that those markers demonstrate collinearity, but SEL volumes performed better (as assesed by a reduced BIC, 156.14 vs 157.10). In addition, when the early onset MS subcohort was explored in the logistic model, a higher risk of CDP was confirmed only when using as explanatory metric SEL (CDP explained by possible SEL log-volume OR = 13.38, 95%CI 1.56 to 114.60, p = 0.018, pseudo-R^2 = 0.25).

4. Discussion

Chronic active lesions in MS provide a plausible explanation for worsening of disability beyond initial lesion formation. In this retrospective observational study, with up to 12 years of follow-up, we found that lesion expansion (SELs) was associated with increasing T1-hypointensity (a marker of axonal damage and demyelination) and with MTR reduction at follow-up (also a marker of both demyelinaton and axonal loss). SELs were associated with disability progression and more widespread neurodegeneration, independent of conventional lesion measures or brain atrophy highlighting their relevance as a therapeutic target in MS.

4.1. SELs are relevant in relapsing-onset MS

We confirm in our study that in relapse-onset MS, SELs are a very common finding, as from 86 to 99% of the total cohort in our study had at least one definite and possible SEL (respectively). We found that between 9% (definite SELs) and 26% (possible SELs) of lesions in the present RRMS cohort showed evidence of chronic activity and that the per patient lesion count was a median of 6 SELs. Using another SEL

analysis technique in relapsing MS trial cohorts, lower counts were reported (median number of SELs = 4.6, proportion of lesions defined as SELs = 8.6%) (Elliott et al., 2019), but the follow-up period in that study was shorter (up to 96 weeks). Using a cluster analysis, we found three sub-populations based on (possible) SEL counts. The majority of patients (48%) had intermediate SEL counts (3 to 10), 29% had high counts (greater than10) and 23% low SEL counts (0 to 2). The clusters of patients with intermediate and high SEL counts had a higher EDSS at last follow-up, and consistent MRI metrics of inflammatory activity (higher baseline T2 lesion volume and T2 lesion counts) and of neurodegenerative activity (lower values in NBV and CGM/DGM volumes). A recent study investigating rims at susceptibility MRI, has similarly identified a classification of patients depending on low versus high number of rims (Absinta et al., 2019). In that study, the authors identified higher percentages (30–40%) of patients without any rims or with low rim counts (Absinta et al., 2019). The overall lower percentages of rims found in MRI longitudinal studies might suggest that only a subset of the chronic active lesions as defined using SEL would develop rims.

4.2. SELs associate to radiological MRI markers of MS neurodegeneration

In this work, multiple MRI markers related to chronic lesions, global and regional brain volumes were analysed in relation to SEL-derived metrics. Recently, fully automatic segmentation techniques have allowed efficient detection of PBHs in MRI studies, promoting a stratification of several lesion subtypes through the assessment of T1 intensity ratio to the surrounding tissues (Giorgio et al., 2014; Spies et al., 2013; Datta et al., 2006; Wu et al., 2006; Khayati et al., 2008; Valcarcel et al., 2018). In our study, PBHs were automatically determined using an in-house developed pipeline, with some similarities to previous studies using T1 intensity ratio evaluation to classify T1 hypointense lesions (Spies et al., 2013; Khayati et al., 2008; Valcarcel et al., 2018; Tam et al., 2011). The association analysis confirmed a relevant positive correlation between SEL counts or SEL log-volumes and PBHs. In addition, higher percentages of PBHs coincided with SELs (52–61% out of the total BHs). Those results imply a link between SELs and PBHs, and suggest an evolution from a chronic active initial stage (SELs) towards

accumulation of higher degree of neuro-axonal damage, typical of PBHs. Conventional MRI markers of neurodegeneration were investigated, and the increase in SEL burden, despite not being correlated to brain atrophy measures, was consistently associated to reductions in global and regional brain volumes (both at baseline and at last follow-up). Those metrics are known to be markers of neurodegenerative activity, associated to higher risk for disability progression (Zivadinov et al., 2016; Rocca et al., 2021; De Stefano et al., 2010; Jacobsen et al., 2014). Therefore, presence of both PBHs and SELs could impact separately, as additive risk factors, to develop a worse clinical outcome in relapsing-onset MS.

4.3. Structural changes in SELs assessed with T1 and MTR

The structural MRI features of SELs were assessed through lesion-level quantitative analyses. In line with previous studies conducted on trial populations, including relapsing and progressive MS patients (Elliott et al., 2017; van Walderveen et al., 1998), in the current study SELs demonstrated a significant T1 intensity reduction over time assessed in a relapse-onset MS cohort predominantly in an early disease stage. Interestingly, the highest T1 intensity ratio change was identified within possible SELs. Similarly, the results of the MTR analysis (lower MTR at follow-up within SELs vs non-SELs) were consistent with previous studies showing that SELs are characterised by microstructural damage (Bramow et al., 2010; Preziosa et al., 2021). In imaging-pathological correlations, T1 and MTR reductions have been associated with neuro-axonal loss (Schmierer et al., 2004), therefore SEL equally present accumulating neuro-axonal damage.

Our results suggest that the possible SEL type could represent an earlier step of the MS lesion evolution. In this dynamic stage, there might be a tendency towards a prevalence of structural variability (possibly due to a mixture of demyelination and remyelination), reflected by higher degree and variability of T1 and MTR changes. Definite SELs could be seen as a later stage of the lesion evolution, when a significant tissue damage is reached (including irreversible neuro-axonal loss), as confirmed by their generally lower MTR values. Overall, accumulation of SELs could drive other pathological processes relevant to MS progression, such as global tissue loss and microstructural lesion damage.

4.4. SELs and clinical outcomes

Higher disability level, as measured by an increase in the EDSS score evolution over time, independently associated to higher SEL volumes (beta = 0.11, p = 0.01), taking into account the demographical and the other relevant MRI measures (T2 lesion volume and brain atrophy) in this relapsing-onset MS cohort. Furthermore, SEL volumes could predict five times higher risk of CDP (OR = 5.15, p = 0.006). Those results imply an active role for SELs in determining a change in clinical outcome, which were confirmed when the analysis was restricted to a subcohort of patients with an early onset MS (≤5 years, n = 85).

Overall, the 'possible' SEL types metrics were better correlated to clinical measures compared to the 'definite' SELs. This result could be interpreted as a higher flexibility for this SEL subtype to represent the dynamic stage of a chronic active lesion, and its higher potential to expand, as an intermediate evolution step of MS lesions. From the SEL pipeline definition, the definite SEL types need to satisfy semi-arbitrary restrictions, which might have not a clear correlation to the patho-biological processes in MS. For example, the definite SEL selection criteria stipulates that there be an homogeneous expansion in all directions but in pathological studies lesion boundaries might also evolve into different shapes, depending on the degree of local and spatial specific chronic demyelination or remyelination [50].

4.5. Methodological limitations and future steps

In this retrospective cohort SEL counts were higher compared to the figures identified in previous trials (up to about 2 years) (Elliott et al., 2019). The result in our study might be related to a longer observation time to the last follow-up MRI scan (reaching up to 12 years) or to the use of less restrictive parameters in SEL definition. Additionally, the SEL pipeline used in this work did not use an arbitrary cut-off of a minimal annualised expansion rate, used in other studies as a further inclusion criteria [51], which may have further increased the number of SELs detected. Currently, there is not a gold standard for SEL identification (or any threshold of minimal expansion), and a study to evaluate different techniques and their sensitivity would benefit an appropriate comparisons of the results.

Another limitation was the absence of post-contrast images, precluding identification of acute contrast enhancing lesions, which may transiently show T1-hypointensity related to oedema. Given that lesions had to remain T1-hypointense over a median follow-up of ~ 3 years, the potential effects of transient T1 hypointensity related to acute inflammation is unlikely to have materially influenced the present results.

Given the retrospective nature of this study the time intervals at each follow-up were variable, and this heterogeneity of the follow-up might have impacted on the overall computation of SELs, which requires the normalization (z-score computation) of the expansion rate within all subjects. However, a further analysis restricted to the early onset MS subcohort, evaluating only patients with disease duration lower or equal than 5 years at baseline, confirmed in our main findings.

As another limitation of the results of the MRI structural analysis regarding the high degree of T1 hypointensity within SEL lesions, a possible bias of the increase in sensitivity stands with the methodology itself, as the deformation field is obtained through the analysis of T1-weighted images. The lower T1 signal in SELs compared to other lesion types is expected to be a consequence of the inclusion criteria as part of the SEL detection algorithm. Moreover, T1-weighted images offer a better resolution and when they were available in 3D acquisition the lesion boundaries were more distinct, and the deformation field computation more precise as compared to the 2D FLAIR/T2-weighted sequences.

Finally, the observation that 'possible' compared with 'definite' SELs correlated more closely with clinical outcomes suggests that either the 'definite' SEL definition overlooks a substantial proportion of clinically relevant SEL activity, or that there are other features to the 'possible' SELs that contribute to their clinical impact. In either case, further work optimising the definitions of SELs would be worthwhile, particularly with a view to better understand the pathophysiological process of the evolution to chronic active lesion stage and to improve their use as an outcome measure in clinical trials.

As a future step, it would be of interest to develop the multi-parametric analysis of SELs further, including other quantitative MRI markers, such as diffusion-weighted MRI and network integrity metrics, and their relationship with the rims at susceptibility MRI, in order to better characterise subtypes of SELs, their impact on the functional global brain level, and how they evolve over time.

4.6. Conclusions

SELs are a common finding in relapse-onset MS. Over time they not only expand, but also show associated T1 and MTR features of pathological progression. Importantly, they correlate independently with clinical outcomes, and therefore might serve as an imaging marker of MS progression. Further work is required to determine if they can help identify a transition from RR or SPMS, which can be clinically challenging, or play a useful role in MS clinical trials, particularly in progressive MS.

5. Disclosures & Funding

6. Data and code availability statement

Researchers interested in accessing the data and the code to run the SEL and PBHs pipelines of this study can contact Prof Frederik Barkhof (f.barkhof@ucl.ac.uk). A data sharing agreement enabling non-commercial research use will be stipulated. The scripts written to process the MRI scans and perform statistical analysis will be shared upon request.

CRediT authorship contribution statement

Alberto Calvi: Conceptualization, Methodology, Software, Formal analysis, Data curation, Writing – original draft, Project administration. **Carmen Tur:** Conceptualization, Formal analysis, Writing – review & editing. **Declan Chard:** Conceptualization, Writing – review & editing. **Jonathan Stutters:** Data curation, Methodology. **Olga Ciccarelli:** Conceptualization, Writing – review & editing. **Rosa Cortese:** Resources, Writing – review & editing. **Marco Battaglini:** Resources. **Anna Pietroboni:** Resources. **Milena De Riz:** Resources. **Daniela Galimberti:** Resources. **Elio Scarpini:** Resources. **Nicola De Stefano:** Conceptualization, Resources. **Ferran Prados:** Conceptualization, Methodology, Software, Formal analysis, Writing – review & editing. **Frederik Barkhof:** Conceptualization, Methodology, Writing – review & editing, Funding acquisition.

Declaration of Competing Interest

Acknowledgements

Appendix A. Supplementary data

Supplementary data to this article can be found online at https://doi.org/10.1016/j.nicl.2022.103048.

References

Prineas, J.W., Parratt, J.D.E., 2012. Oligodendrocytes and the early multiple sclerosis lesion. Ann Neurol. 72 (1), 18–31. https://doi.org/10.1002/ana.23634.

Prineas, J.W., Kwon, E.E., Cho, E.-S., Sharer, L.R., Barnett, M.H., Oleszak, E.L., Hoffman, B., Morgan, B.P., 2001. Immunopathology of secondary-progressive multiple sclerosis. Ann Neurol. 50 (5), 646–657.

Thompson, A.J., Baranzini, S.E., Geurts, J., Hemmer, B., Ciccarelli, O., 2018. Multiple sclerosis. Lancet. 391 (10130), 1622–1636. https://doi.org/10.1016/S0140-6736(18)30481-1.

Barkhof, F., Brück, W., De Groot, C.J.A., Bergers, E., Hulshof, S., Geurts, J., Polman, C.H., van der Valk, P., 2003. Remyelinated Lesions in Multiple Sclerosis. Arch Neurol. 60 (8), 1073.

Kuhlmann, T., Ludwin, S., Prat, A., Antel, J., Brück, W., Lassmann, H., 2017. An updated histological classification system for multiple sclerosis lesions. Acta Neuropathol. 133, 13–24. https://doi.org/10.1007/s00401-016-1653-y.

Frischer, J.M., Bramow, S., Dal-Bianco, A., Lucchinetti, C.F., Rauschka, H., Schmidbauer, M., Laursen, H., Sorensen, P.S., Lassmann, H., 2009. The relation between inflammation and neurodegeneration in multiple sclerosis brains. Brain. 132 (5), 1175–1189.

Lassmann, H., 2019. Pathogenic Mechanisms Associated With Different Clinical Courses of Multiple Sclerosis. Front Immunol. 9, 3116. https://doi.org/10.3389/fimmu.2018.03116.

Luchetti, S., Fransen, N.L., van Eden, C.G., Ramaglia, V., Mason, M., Huitinga, I., 2018. Progressive multiple sclerosis patients show substantial lesion activity that correlates with clinical disease severity and sex: a retrospective autopsy cohort analysis. Acta Neuropathol. 135 (4), 511–528. https://doi.org/10.1007/s00401-018-1818-y.

Frischer, J.M., Weigand, S.D., Guo, Y., Kale, N., Parisi, J.E., Pirko, I., Mandrekar, J., Bramow, S., Metz, I., Brück, W., Lassmann, H., Lucchinetti, C.F., 2015. Clinical and pathological insights into the dynamic nature of the white matter multiple sclerosis plaque. Ann Neurol. 78 (5), 710–721.

van Walderveen, M.A.A., Kamphorst, W., Scheltens, P., van Waesberghe, J.H.T.M., Ravid, R., Valk, J., Polman, C.H., Barkhof, F., 1998. Histopathologic correlate of hypointense lesions on T1-weighted spin-echo MRI in multiple sclerosis. Neurology. 50 (5), 1282–1288.

Van Waesberghe, J.H.T.M., Kamphorst, W., De Groot, C.J.A., et al., 1999. Axonal loss in multiple sclerosis lesions: Magnetic resonance imaging insights into substrates of disability. Ann Neurol. 46 (5), 747–754. https://doi.org/10.1002/1531-8249(199911)46:5<747::AID-ANA10>3.0.CO;2-4.

Schmierer, K., Scaravilli, F., Altmann, D.R., Barker, G.J., Miller, D.H., 2004. Magnetization transfer ratio and myelin in postmortem multiple sclerosis brain. Ann Neurol. 56 (3), 407–415. https://doi.org/10.1002/ana.20202.

Kapoor, R., Furby, J., Hayton, T., Smith, K.J., Altmann, D.R., Brenner, R., Chataway, J., Hughes, R.A.C., Miller, D.H., 2010. Lamotrigine for neuroprotection in secondary progressive multiple sclerosis: a randomised, double-blind, placebo-controlled, parallel-group trial. Lancet Neurol. 9 (7), 681–688.

Molyneux, P.D., Brex, P.A., Fogg, C., et al., 2000. The precision of TI hypointense lesion volume quantification in multiple sclerosis treatment trials: A multicenter study. Mult Scler. 6 (4), 237–240. https://doi.org/10.1177/135245850000600405.

van den Elskamp, I.J., Lembcke, J., Dattola, V., Beckmann, K., Pohl, C., Hong, W., Sandbrink, R., Wagner, K., Knol, D.L., Uitdehaag, B., Barkhof, F., 2008. Persistent T1 hypointensity as an MRI marker for treatment efficacy in multiple sclerosis. Mult Scler. 14 (6), 764–769.

Bagnato, F., Jeffries, N., Richert, N.D., et al., 2003. Evolution of T1 black holes in patients with multiple sclerosis imaged monthly for 4 years. Brain. 126 (8), 1782–1789. https://doi.org/10.1093/BRAIN/AWG182.

Truyen, L., van Waesberghe, J.H.T.M., van Walderveen, M.A.A., van Oosten, B.W., Polman, C.H., Hommes, O.R., Ader, H.J.A., Barkhof, F., 1996. Accumulation of hypointense lesions ('black holes') on T1 spin-echo MRI correlates with disease progression in multiple sclerosis. 47 (6), 1469–1476.

van Walderveen, M.A.A., Lycklama à Nijeholt, G.J., Adèr, H.J., Jongen, P.J.H., Polman, C.H., Castelijns, J.A., Barkhof, F., 2001. Hypointense lesions on T1-weighted spin-echo magnetic resonance imaging: Relation to clinical characteristics

in subgroups of patients with multiple sclerosis. Arch Neurol. 58 (1) https://doi.org/10.1001/archneur.58.1.76.

Sailer, M., Losseff, N.A., Wang, L., Gawne-Cain, M.L., Thompson, A.J., Miller, D.H., 2001. T1 lesion load and cerebral atrophy as a marker for clinical progression in patients with multiple sclerosis. A prospective 18 months follow-up study. Eur J Neurol. 8 (1), 37–42. https://doi.org/10.1046/j.1468-1331.2001.00147.x.

Elliott, C., Wolinsky, J., Hauser, J., et al., 2017. Detection and characterisation of slowly evolving lesions in multiple sclerosis using conventional brain MRI. Mult Scler J. 23 (3_suppl), 52. https://doi.org/10.1177/1352458517731283.

Dal-Bianco, A., Grabner, G., Kronnerwetter, C., Weber, M., Höftberger, R., Berger, T., Auff, E., Leutmezer, F., Trattnig, S., Lassmann, H., Bagnato, F., Hametner, S., 2017. Slow expansion of multiple sclerosis iron rim lesions: pathology and 7 T magnetic resonance imaging. Acta Neuropathol. 133 (1), 25–42.

Vrenken, H., Jenkinson, M., Horsfield, M.A., Battaglini, M., van Schijndel, R.A., Rostrup, E., Geurts, J.J.G., Fisher, E., Zijdenbos, A., Ashburner, J., Miller, D.H., Filippi, M., Fazekas, F., Rovaris, M., Rovira, A., Barkhof, F., de Stefano, N., 2013. Recommendations to improve imaging and analysis of brain lesion load and atrophy in longitudinal studies of multiple sclerosis. J Neurol. 260 (10), 2458–2471.

Elliott, C., Belachew, S., Wolinsky, J.S., Hauser, S.L., Kappos, L., Barkhof, F., Bernasconi, C., Fecker, J., Model, F., Wei, W., Arnold, D.L., 2019. Chronic white matter lesion activity predicts clinical progression in primary progressive multiple sclerosis. Brain. 142 (9), 2787–2799.

Elliott C, Arnold DL, Chen H, et al. Patterning Chronic Active Demyelination in Slowly Expanding/Evolving White Matter MS Lesions. *Am J Neuroradiol.* 2020;41(9):1584-1591. doi:10.3174/AJNR.A6742.

Calvi, A., Carrasco, F.P., Tur, C., Chard, D.T., Stutters, J., De Angelis, F., John, N., Williams, T., Doshi, A., Samson, R.S., MacManus, D., Gandini Wheeler-Kingshott, C. A., Ciccarelli, O., Chataway, J., Barkhof, F., 2022. Association of Slowly Expanding Lesions on MRI With Disability in People With Secondary Progressive Multiple Sclerosis. Neurology 98 (17), e1783–e1793.

Thompson, A.J., Banwell, B.L., Barkhof, F., Carroll, W.M., Coetzee, T., Comi, G., Correale, J., Fazekas, F., Filippi, M., Freedman, M.S., Fujihara, K., Galetta, S.L., Hartung, H.P., Kappos, L., Lublin, F.D., Marrie, R.A., Miller, A.E., Miller, D.H., Montalban, X., Mowry, E.M., Sorensen, P.S., Tintoré, M., Traboulsee, A.L., Trojano, M., Uitdehaag, B.M.J., Vukusic, S., Waubant, E., Weinshenker, B.G., Reingold, S.C., Cohen, J.A., 2018. Diagnosis of multiple sclerosis: 2017 revisions of the McDonald criteria. Lancet Neurol. 17 (2), 162–173.

Kurtzke, J.F., 1983. Rating neurologic impairment in multiple sclerosis: An expanded disability status scale (EDSS), 1444 1444 Neurology. 33 (11). https://doi.org/10.1212/WNL.33.11.1444.

Lublin, F., Miller, D.H., Freedman, M.S., Cree, B.A.C., Wolinsky, J.S., Weiner, H., Lubetzki, C., Hartung, H.-P., Montalban, X., Uitdehaag, B.M.J., Merschhemke, M., Li, B., Putzki, N., Liu, F.C., Häring, D.A., Kappos, L., 2016. Oral fingolimod in primary progressive multiple sclerosis (INFORMS): a phase 3, randomised, double-blind, placebo-controlled trial. The Lancet 387 (10023), 1075–1084.

Hickman, S.J., Barker, G.J., Molyneux, P.D., Miller, D.H., 2002. Technical note: The comparison of hypointense lesions from "pseudo-T1" and T1-weighted images in secondary progressive multiple sclerosis. Mult Scler. 8 (5), 433–435. https://doi.org/10.1191/1352458502ms824xx.

Cardoso, M.J., Modat, M., Wolz, R., Melbourne, A., Cash, D., Rueckert, D., Ourselin, S., 2015. Geodesic Information Flows: Spatially-Variant Graphs and Their Application to Segmentation and Fusion. IEEE Trans Med Imaging. 34 (9), 1976–1988.

Prados, F., Cardoso, M.J., Kanber, B., Ciccarelli, O., Kapoor, R., Gandini Wheeler-Kingshott, C.A.M., Ourselin, S., 2016. A multi-time-point modality-agnostic patch-based method for lesion filling in multiple sclerosis. Neuroimage. 139, 376–384.

Smith, S.M., Zhang, Y., Jenkinson, M., Chen, J., Matthews, P.M., Federico, A., De Stefano, N., 2002. Accurate, robust, and automated longitudinal and cross-sectional brain change analysis. Neuroimage. 17 (1), 479–489.

Elliott, C., Wolinsky, J.S., Hauser, S.L., Kappos, L., Barkhof, F., Bernasconi, C., Wei, W., Belachew, S., Arnold, D.L., 2019. Slowly expanding/evolving lesions as a magnetic resonance imaging marker of chronic active multiple sclerosis lesions. Mult Scler J. 25 (14), 1915–1925.

Absinta, M., Sati, P., Masuzzo, F., Nair, G., Sethi, V., Kolb, H., Ohayon, J., Wu, T., Cortese, I.C.M., Reich, D.S., 2019. Association of Chronic Active Multiple Sclerosis Lesions With Disability In Vivo. JAMA Neurol. 76 (12), 1474.

Giorgio, A., Stromillo, M.L., Bartolozzi, M.L., Rossi, F., Battaglini, M., De Leucio, A., Guidi, L., Maritato, P., Portaccio, E., Sormani, M.P., Amato, M.P., De Stefano, N., 2014. Relevance of hypointense brain MRI lesions for long-term worsening of clinical disability in relapsing multiple sclerosis. Mult Scler. 20 (2), 214–219.

Spies, L., Tewes, A., Suppa, P., Opfer, R., Buchert, R., Winkler, G., Raji, A., 2013. Fully automatic detection of deep white matter T1 hypointense lesions in multiple sclerosis. Phys Med Biol. 58 (23), 8323–8337.

Datta, S., Sajja, B.R., He, R., Wolinsky, J.S., Gupta, R.K., Narayana, P.A., 2006. Segmentation and quantification of black holes in multiple sclerosis. Neuroimage. 29 (2), 467–474. https://doi.org/10.1016/j.neuroimage.2005.07.042.

Wu, Y., Warfield, S.K., Tan, I.L., Wells, W.M., Meier, D.S., van Schijndel, R.A., Barkhof, F., Guttmann, C.R.G., 2006. Automated segmentation of multiple sclerosis lesion subtypes with multichannel MRI. Neuroimage. 32 (3), 1205–1215.

Khayati, R., Vafadust, M., Towhidkhah, F., Nabavi, S.M., 2008. A novel method for automatic determination of different stages of multiple sclerosis lesions in brain MR FLAIR images. Comput Med Imaging Graph. 32 (2), 124–133. https://doi.org/10.1016/j.compmedimag.2007.10.003.

Valcarcel, A.M., Linn, K.A., Khalid, F., Vandekar, S.N., Tauhid, S., Satterthwaite, T.D., Muschelli, J., Martin, M.L., Bakshi, R., Shinohara, R.T., 2018. A dual modeling approach to automatic segmentation of cerebral T2 hyperintensities and T1 black holes in multiple sclerosis. NeuroImage Clin. 20, 1211–1221.

Tam, R.C., Traboulsee, A., Riddehough, A., Sheikhzadeh, F., Li, D., 2011. The impact of intensity variations in T1-hypointense lesions on clinical correlations in multiple sclerosis. Mult Scler J. 17 (8), 949–957. https://doi.org/10.1177/1352458511402113.

Zivadinov, R., Uher, T., Hagemeier, J., Vaneckova, M., Ramasamy, D.P., Tyblova, M., Bergsland, N., Seidl, Z., Dwyer, M.G., Krasensky, J., Havrdova, E., Horakova, D., 2016. A serial 10-year follow-up study of brain atrophy and disability progression in RRMS patients. Mult Scler 22 (13), 1709–1718.

Rocca, M.A., Valsasina, P., Meani, A., Gobbi, C., Zecca, C., Rovira, A., Sastre-Garriga, J., Kearney, H., Ciccarelli, O., Matthews, L., Palace, J., Gallo, A., Bisecco, A., Lukas, C., Bellenberg, B., Barkhof, F., Vrenken, H., Preziosa, P., Filippi, M., 2021. Association of Gray Matter Atrophy Patterns with Clinical Phenotype and Progression in Multiple Sclerosis. Neurology. 96 (11), e1561–e1573.

De Stefano, N., Giorgio, A., Battaglini, M., Rovaris, M., Sormani, M.P., Barkhof, F., Korteweg, T., Enzinger, C., Fazekas, F., Calabrese, M., Dinacci, D., Tedeschi, G., Gass, A., Montalban, X., Rovira, A., Thompson, A., Comi, G., Miller, D.H., Filippi, M., 2010. Assessing brain atrophy rates in a large population of untreated multiple sclerosis subtypes. Neurology. 74 (23), 1868–1876.

Jacobsen, C., Hagemeier, J., Myhr, K.-M., Nyland, H., Lode, K., Bergsland, N., Ramasamy, D.P., Dalaker, T.O., Larsen, J.P., Farbu, E., Zivadinov, R., 2014. Brain atrophy and disability progression in multiple sclerosis patients: A 10-year follow-up study. J Neurol Neurosurg Psychiatry. 85 (10), 1109–1115.

van Walderveen, M.A.A., Kamphorst, W., Scheltens, P., van Waesberghe, J.H.T.M., Ravid, R., Valk, J., Polman, C.H., Barkhof, F., 1998. Histopathologic correlate of hypointense lesions on T1-weighted spin- echo MRI in multiple sclerosis. Neurology. 50 (5), 1282–1288.

Bramow, S., Frischer, J.M., Lassmann, H., Koch-Henriksen, N., Lucchinetti, C.F., Sørensen, P.S., Laursen, H., 2010. Demyelination versus remyelination in progressive multiple sclerosis. A J Neurol. 133 (10), 2983–2998.

Preziosa, P., Pagani, E., Moiola, L., Rodegher, M., Filippi, M., Rocca, M.A., 2021. Occurrence and microstructural features of slowly expanding lesions on fingolimod or natalizumab treatment in multiple sclerosis. Mult Scler J. 27 (10), 1520–1532.